Hindawi Publishing Corporation
Journal of Nanomaterials
Volume 2013, Article ID 891365, 6 pages
http://dx.doi.org/10.1155/2013/891365

Research Article

Annealing Effects of Sputtered Cu_2O Nanocolumns on ZnO-Coated Glass Substrate for Solar Cell Applications

Lung-Chien Chen,[1] Chung-Chieh Wang,[2] and Suz-Wei Lu[1]

[1] *Department of Electro-Optical Engineering, National Taipei University of Technology, No. 1, Section 3, Chung-Hsiao E. Road, Taipei 106, Taiwan*
[2] *Materials & Electro-Optics Research Division, Chung-Shan Institute of Science and Technology, P.O. Box No. 90008-8-6, Lung Tan, Taoyuan 325, Taiwan*

Correspondence should be addressed to Lung-Chien Chen; ocean@ntut.edu.tw

Received 19 December 2012; Revised 5 February 2013; Accepted 13 February 2013

Academic Editor: Sanqing Huang

Cuprous oxide (Cu_2O) films were prepared on an indium tin oxide glass substrate by radiofrequency magnetron sputtering using a high-purity Cu target. The temperature of annealing was varied to obtain Cu_2O thin films with various elements, compositions, and surface structures. The p-Cu_2O thin films thus formed were characterized by FESEM and XRD. After annealing at 500°C, the bilayer structure which consisted of Cu nanoclusters on the surface of a film of Cu_2O nanocolumns was observed. The Cu_2O solar cell with the bilayered structure exhibited poor power conversion efficiency.

1. Introduction

Cuprous oxide (Cu_2O) is a potential oxide semiconductor with a direct band gap of 2.17 eV because the theoretical energy conversion efficiency of a Cu_2O solar cell is of the order of 20% [1–3]. Undoped Cu_2O, prepared by various techniques, is usually a p-type semiconducting material because of its native defects that are formed by Cu vacancies [4, 5]. Cu_2O is of a nontoxic nature and is an attractive all-oxide candidate for low-cost photovoltaic (PV) applications. Cu_2O has long been considered to be an attractive transparent conductor oxide (TCO) semiconductor, which is favorable for the fabrication of low-cost solar cells for terrestrial applications. Several groups have reportedly developed p-n junction solar cells with a TCO/Cu_2O heterostructure, such as zinc oxide (ZnO)/Cu_2O, indium-doped ZnO (IZO)/Cu_2O, aluminum-doped ZnO (AZO)/Cu_2O, and gallium-doped ZnO (GZO)/Cu_2O heterojunction [6–11]. Cu_2O thin films have been prepared by various methods, including reactive sputtering [12], metal-organic chemical vapor deposition (MOCVD) [13], electrochemical deposition [14–17], chemical dissolution [18–20], and the direct oxidation of Cu sheets [21].

According to the literature, the performance of Cu_2O-based solar cells is significantly affected by the crystallinity of Cu_2O, because Cu metal can easily be formed at the surface of the Cu_2O films or at the interface between the TCO and the Cu_2O films when thin films of TCO are deposited on the Cu_2O films. Therefore, this study investigates the deposition of the Cu_2O thin films by the magnetron sputtering method; in particular, it examines the effect of changing the temperature of annealing to vary the crystal quality of the Cu_2O thin films.

2. Experimental

In this study, Cu_2O films were prepared on ITO glass using a Cu target with 99.995% purity and a radiofrequency magnetron sputtering system. The Cu targets were in Ar (flow rate of 40 sccm) and O_2 (flow rate of 1–3 sccm) gas at a stable pressure of 3×10^{-3} Torr, and the temperature and time of annealing varied to yield Cu_2O thin films with various properties. The flow rates of both argon and oxygen gases were individually monitored using mass flow controllers.

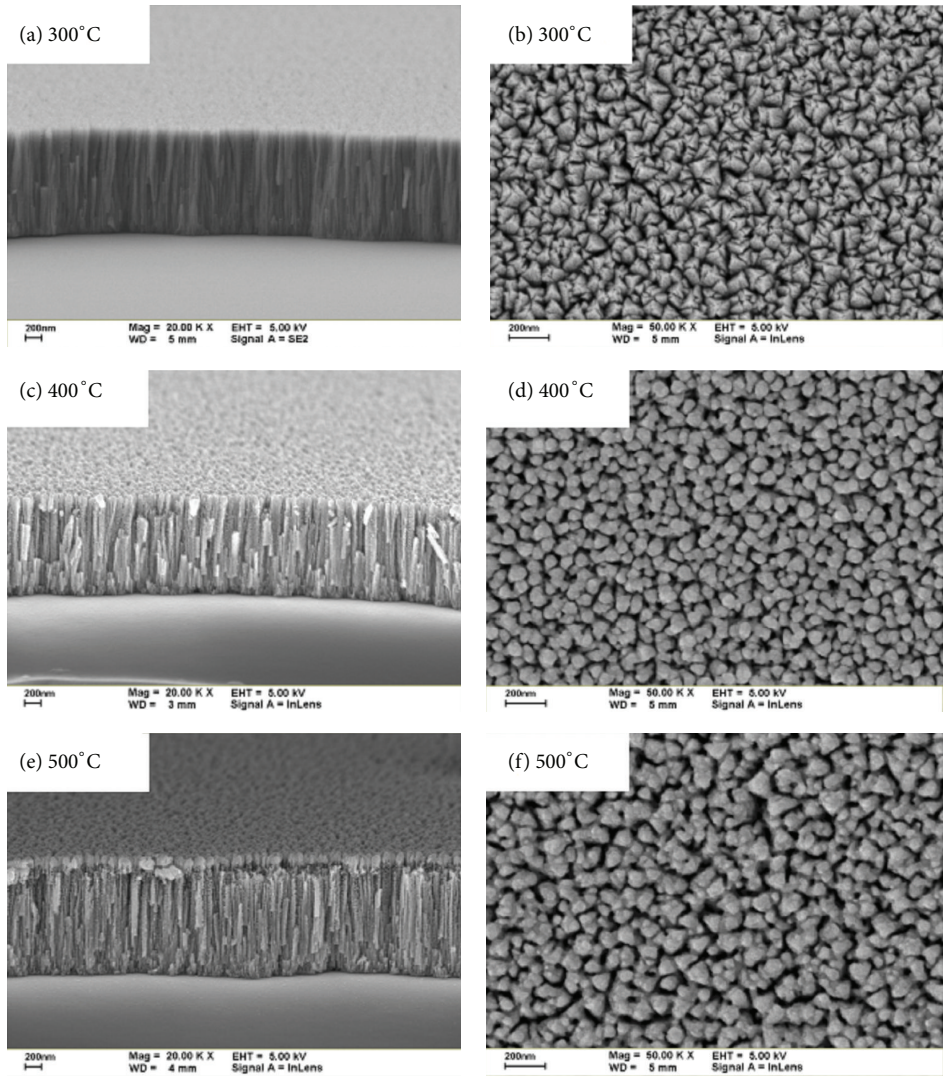

Figure 1: Top-view and cross-sectional FESEM images of microstructures of Cu_2O films following annealing at 300, 400, and 500°C.

Table 1 presents in detail the parameters of reactive magnetron sputtering for the preparation of Cu_2O films. The elements, composition, and surface structure of Cu_2O thin films were characterized by field emission scanning electron microscopy (FESEM) and XRD measurements. The mobility and carrier concentrations in the Cu_2O thin films, and the resistances of the the films, were determined by making Hall measurements.

After the Cu_2O films had been studied, ZnO/Cu_2O heterostructure solar cells were fabricated. A ZnO film and then a Cu_2O film were deposited on an ITO-coated glass substrate. Next, copper electrodes were formed by sputtering onto the surfaces of both of the ZnO film and the Cu_2O film to complete the fabrication of the ZnO/Cu_2O heterostructure solar cells. The current density-voltage (J-V) characteristics were measured using a Keithley 2420 programmable source meter under irradiation by a 100 W xenon lamp. Finally, the irradiation power density on the surface of the sample was calibrated at 100 W/m^2.

Table 1: Sputtering parameters for Cu_2O films.

RF power of Cu target	50 W
Working pressure	4.3×10^{-3} Torr
Annealing temperatures	300–500°C
Flow rate of argon	50 sccm
Flow rate of oxygen	1–3 sccm
Film thickness	800–1000 nm

3. Results and Discussion

Figure 1 shows the top-view and cross-sectional FESEM images of the microstructures of the Cu_2O films that had been annealed at 300, 400, and 500°C. Two-dimensional grain boundaries of the Cu_2O films that were annealed at 400 and 500°C are clearly observed. The oxide scales on the sample that was annealed at 300°C exhibit compact clusters

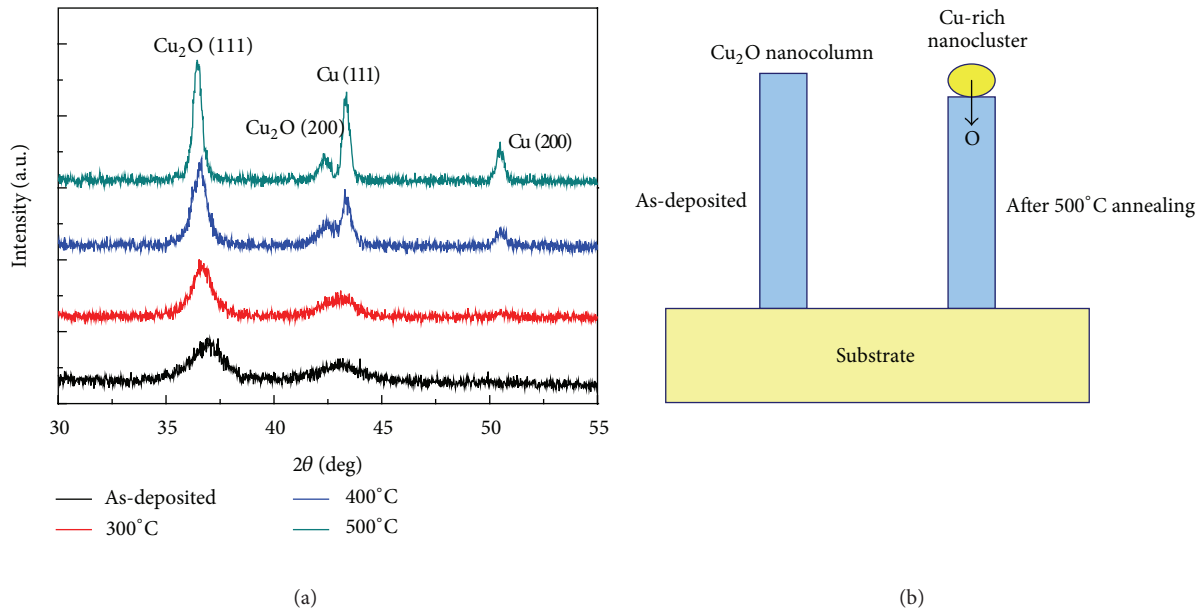

Figure 2: X-ray diffraction patterns of samples that had been annealed at various temperatures.

of fine grains, as shown in Figures 1(a) and 1(b). When the annealing temperature exceeded 400°C, porous, thin oxides formed, particularly developed in the grain boundary regions, implying that they were produced by fast diffusion processes, as shown in Figures 1(c) to 1(e), which may be responsible for the low value of the activation energy. Nanosize grains with sizes from 30 to 50 nm were obtained by varying the annealing temperature and flow rate of oxygen gas. After annealing at 500°C, as shown in Figure 1(e), the bilayer structure consisted of Cu nanoclusters on the surface of a film of Cu nanocolumns was observed.

To elucidate the annealing mechanism, the phase was identified. Figure 2(a) presents the XRD pattern of the Cu_2O films that were treated at various annealing temperatures. XRD diffraction shows that single phase of Cu_2O films was formed by growth at different annealing temperatures, yielding diffraction peaks at 36.45° and 42.33° that corresponded to the (111) and (200) planes of the cubic-structured Cu_2O. At high annealing temperatures, the Cu_2O(111) peak increased and Cu peaks appeared at 400 and 500°C. The Cu_2O(111) peak shifted slightly from 36.45° to 36.93°. The outgassing of oxygen from the surface of the film into the Cu_2O nanocolumns and the formation of Cu clusters on the surface of the Cu_2O film may have contributed to the appearance of the Cu peaks and the shift of the Cu_2O peaks. Figure 2(b) presents the mechanism of formation of the Cu-Cu_2O bilayer.

Figure 3 plots both the resistivity and the mobility as functions of thermal annealing temperature for annealing periods of 10 and 20 min. The sample that was annealed for 10 min had superior electrical characteristics than the sample that had been annealed for 20 min. As the thermal annealing temperature increased, the resistivity of Cu_2O films linearly fell while the mobility declined to ~2–4 cm^2/Vs. The

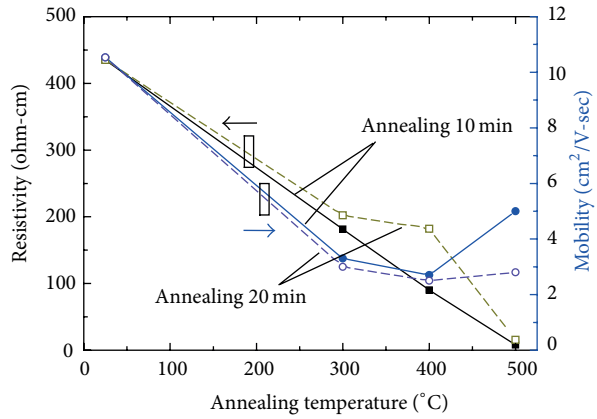

Figure 3: Carrier concentration and mobility as functions of annealing temperature.

reduction of resistivity of the Cu_2O films after annealing may be attributed to the segregation of the Cu-rich nanoclusters from the Cu_2O film, which is shown in Figure 1(e). Also, unlike other studies, a film with relatively low mobility was obtained by postthermal annealing [22–24]. The reduction of mobility in Figure 3 is attributable to the transportation of carriers from one nanocolumn to another nanocolumn. However, as the annealing temperature increased to 500°C, the mobility in the sample that had been annealed for 10 min increased by ~5 cm^2/Vs owing to the increase in the size of the grains in the Cu_2O nanocolumns and the Cu-rich nanoclusters.

Figure 4(a) presents the absorption measurements for the Cu_2O layers following postannealing treatment at various temperatures for 10 min. The layers absorb very strongly

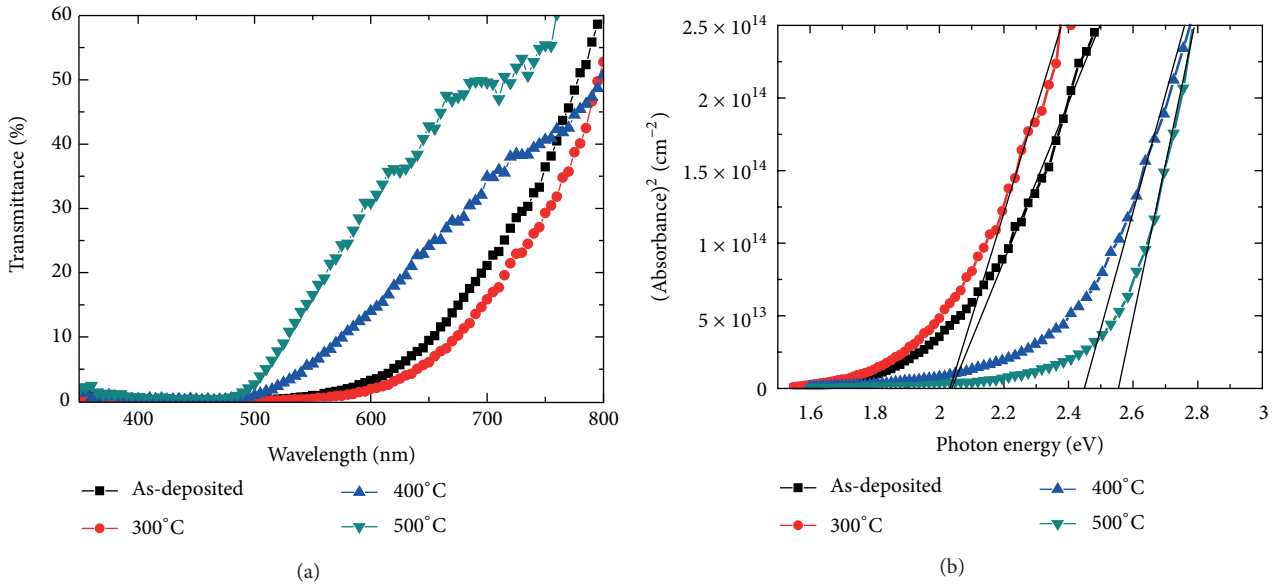

FIGURE 4: Absorbance spectra of (a) Cu_2O films with thermal oxidation at various temperatures and (b) absorption squared as a function of photon energy.

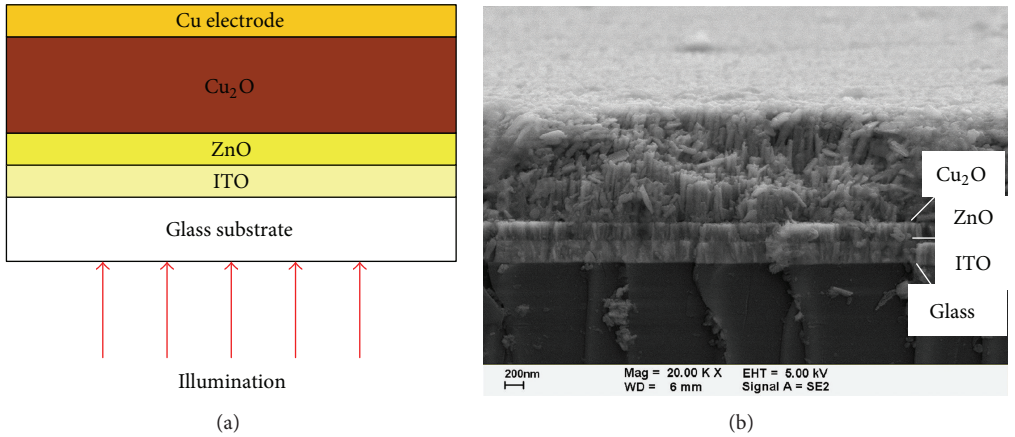

FIGURE 5: (a) Cross-section of completed structure and (b) FESEM image of completed structure.

in the visible region, and so they are favorable materials for use in solar energy devices. According to this figure, the absorption increased continuously with the annealing temperature from 300 to 500°C owing to a drop in Cu content. Figure 4(b) plots absorption squared as a function of photon energy as determined from the transmittance in Figure 4(a). The as-deposited sample and the sample that was postannealed at 300°C had an absorption edge at ~2.1 eV. This value is consistent with other results for the band-gap energy of Cu_2O that can be found in the literature [25–27]. The extrapolation of the linear region of the curves to the horizontal axis gives the band-gap energies of Cu_2O following postannealing at 400 and 500°C, which are ~2.45 and ~2.55 eV, respectively. This result may be attributed to the incorporation of a larger amount of oxygen in the film, making it nonstoichiometric following postannealing. A nonstoichiometric Cu_2O film with higher oxygen content has a smaller lattice constant, a larger band gap, and a higher resistivity.

Figure 5(a) displays the cross-section of the completed structure and Figure 5(b) shows the FESEM image of the structure. The Cu_2O nanocolumns collapse in the image following the preparation of the sample for FESEM observation. Figure 6 plots the J-V characteristics of the ZnO/Cu_2O heterostructure with and without illumination. The cell performance was measured under AM 1.5 illumination with a solar intensity of 100 mW/cm^2 at 25°C. The cell had an active area of 0.3×0.3 cm^2 and no antireflective coating. ZnO/Cu_2O solar cells exhibited the following static parameters; J_{sc} of 0.0325 mA/cm^2, V_{oc} of 0.1 V, FF of 0.283, and a conversion efficiency (η) of 0.092%. The low FF value and poor conversion efficiency are caused by the high series resistance and low

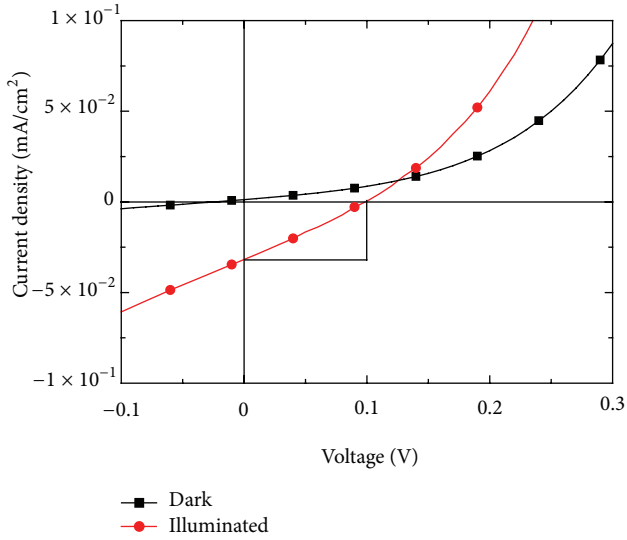

FIGURE 6: J-V curves of IZO/Cu_2O heterostructure solar cells in dark and under illumination.

shunt resistance. The series resistance is caused mainly by the Cu_2O structure that is formed from the nanocolumns, which degrades carrier transport. The shunt resistance is produced by charge leakage from the edges of the Cu_2O nanocolumns.

4. Conclusions

Cuprous oxide (Cu_2O) films were prepared on an indium tin oxide glass substrate by radiofrequency magnetron sputtering using a highly pure Cu target. The bilayer structure comprised Cu nanoclusters on the surface of Cu_2O nanocolumns film following annealing at 500°C. The measured parameters of the cells were the short-circuit current density (J_{sc}), the open-circuit voltage (V_{oc}), and the efficiency (η), with values of 0.0325 mA/cm^2, 0.1 V, and 0.092%, respectively. The Cu_2O solar cell with the bilayer structure had a poor power conversion efficiency because of the nanocolumn structure.

Acknowledgment

Financial support of this paper was provided by the National Science Council of the Republic of China under Contract no. NSC 101-2221-E-027-054.

References

[1] L. C. Olsen, F. W. Addis, and W. Miller, "Experimental and theoretical studies of Cu_2O solar cells," *Solar Cells*, vol. 7, no. 3, pp. 247–279, 1982.

[2] B. P. Rai, "Cu_2O solar cells: a review," *Solar Cells*, vol. 25, no. 3, pp. 265–272, 1988.

[3] A. A. Berezin and F. L. Weichman, "Photovoltaic effect in cuprous oxide-copper junctions in relation to the optical absorption spectrum of cuprous oxide," *Solid State Communications*, vol. 37, no. 2, pp. 157–160, 1981.

[4] M. Nolan and S. D. Elliott, "The p-type conduction mechanism in Cu_2O: a first principles study," *Physical Chemistry Chemical Physics*, vol. 8, no. 45, pp. 5350–5358, 2006.

[5] M. Sieberer, J. Redinger, and P. Mohn, "Electronic and magnetic structure of cuprous oxide Cu_2O doped with Mn, Fe, Co, and Ni: a density-functional theory study," *Physical Review B*, vol. 75, no. 3, Article ID 035203, 2007.

[6] J. Cui and U. J. Gibson, "A simple two-step electrodeposition of Cu_2O/ZnO Nanopillar solar cells," *Journal of Physical Chemistry C*, vol. 114, no. 14, pp. 6408–6412, 2010.

[7] T. Minami, T. Miyata, K. Ihara, Y. Minamino, and S. Tsukada, "Effect of ZnO film deposition methods on the photovoltaic properties of ZnO-Cu_2O heterojunction devices," *Thin Solid Films*, vol. 494, no. 1-2, pp. 47–52, 2006.

[8] C. C. Chen, L. C. Chen, and Y. H. Lee, "Fabrication and optoelectrical properties of IZO/Cu_2O heterostructure solar cells by thermal oxidation," *Advances in Condensed Matter Physics*, vol. 2012, Article ID 129139, 5 pages, 2012.

[9] W. Septina, S. Ikeda, M. A. Khan et al., "Potentiostatic electrodeposition of cuprous oxide thin films for photovoltaic applications," *Electrochimica Acta*, vol. 56, no. 13, pp. 4882–4888, 2011.

[10] X. Wang, R. Li, and D. Fan, "Nanostructured Al-ZnO/CdSe/Cu_2O ETA solar cells on Al-ZnO film/quartz glass templates," *Nanoscale Research Letters*, vol. 6, article 614, 2011.

[11] L. M. Wong, S. Y. Chiam, J. Q. Huang, S. J. Wang, J. S. Pan, and W. K. Chim, "Growth of Cu_2O on Ga-doped ZnO and their interface energy alignment for thin film solar cells," *Journal of Applied Physics*, vol. 108, no. 3, Article ID 033702, 2010.

[12] S. Ishizuka, S. Kato, T. Maruyama, and K. Akimoto, "Nitrogen doping into Cu_2O thin films deposited by reactive radio-frequency magnetron sputtering," *Japanese Journal of Applied Physics*, vol. 40, no. 4, pp. 2765–2768, 2001.

[13] S. Jeong and E. S. Aydil, "Heteroepitaxial growth of Cu_2O thin film on ZnO by metal organic chemical vapor deposition," *Journal of Crystal Growth*, vol. 311, no. 17, pp. 4188–4192, 2009.

[14] K. Nakaoka and K. Ogura, "Electrochemical preparation of p-type cupric and cuprous oxides on platinum and gold substrates from copper(II) solutions with various amino acids," *Journal of the Electrochemical Society*, vol. 149, no. 11, pp. C579–C585, 2002.

[15] A. K. Mukhopadhyay, A. K. Chakraborty, A. P. Chatterjee, and S. K. Lahiri, "Galvanostatic deposition and electrical characterization of cuprous oxide thin films," *Thin Solid Films*, vol. 209, no. 1, pp. 92–96, 1992.

[16] S. Joseph and P. V. Kamath, "Electrochemical deposition of Cu_2O on stainless steel substrates: promotion and suppression of oriented crystallization," *Solid State Sciences*, vol. 10, no. 9, pp. 1215–1221, 2008.

[17] T. Fujiwara, T. Nakaue, and M. Yoshimura, "Direct fabrication and patterning of Cu_2O film by local electrodeposition method," *Solid State Ionics*, vol. 175, no. 1–4, pp. 541–544, 2004.

[18] L. Zhang, H. Li, Y. Ni, J. Li, K. Liao, and G. Zhao, "Porous cuprous oxide microcubes for non-enzymatic amperometric hydrogen peroxide and glucose sensing," *Electrochemistry Communications*, vol. 11, no. 4, pp. 812–815, 2009.

[19] C. H. Kuo and M. H. Huang, "Fabrication of truncated rhombic dodecahedral Cu_2O nanocages and nanoframes by particle aggregation and acidic etching," *Journal of the American Chemical Society*, vol. 130, no. 38, pp. 12815–12820, 2008.

[20] G. Jimenez-Cadena, E. Comini, M. Ferroni, and G. Sberveglieri, "Synthesis of Cu_2O bi-pyramids by reduction of $Cu(OH)_2$ in solution," *Materials Letters*, vol. 64, no. 3, pp. 469–471, 2010.

[21] A. Mittiga, E. Salza, F. Sarto, M. Tucci, and R. Vasanthi, "Heterojunction solar cell with 2% efficiency based on a Cu_2O substrate," *Applied Physics Letters*, vol. 88, no. 16, Article ID 163502, 2006.

[22] S. Jeong and E. S. Aydil, "Structural and electrical properties of Cu_2O thin films deposited on ZnO by metal organic chemical vapor deposition," *Journal of Vacuum Science and Technology A*, vol. 28, no. 6, pp. 1338–1343, 2010.

[23] B. S. Li, K. Akimoto, and A. Shen, "Growth of Cu_2O thin films with high hole mobility by introducing a low-temperature buffer layer," *Journal of Crystal Growth*, vol. 311, no. 4, pp. 1102–1105, 2009.

[24] S. Ishizuka, T. Maruyama, and K. Akimoto, "Thin-film deposition of Cu_2O by reactive radio-frequency magnetron sputtering," *Japanese Journal of Applied Physics*, vol. 39, no. 8A, pp. L786–L788, 2000.

[25] J. H. Hsieh, P. W. Kuo, K. C. Peng, S. J. Liu, J. D. Hsueh, and S. C. Chang, "Opto-electronic properties of sputter-deposited Cu_2O films treated with rapid thermal annealing," *Thin Solid Films*, vol. 516, no. 16, pp. 5449–5453, 2008.

[26] V. Figueiredo, E. Elangovan, G. Gonçalves et al., "Electrical, structural and optical characterization of copper oxide thin films as a function of post annealing temperature," *Physica Status Solidi (A)*, vol. 206, no. 9, pp. 2143–2148, 2009.

[27] S. Hussain, C. Cao, G. Nabi, W. S. Khan, Z. Usman, and T. Mahmood, "Effect of electrodeposition and annealing of ZnO on optical and photovoltaic properties of the p-Cu_2O/n-ZnO solar cells," *Electrochimica Acta*, vol. 56, no. 24, pp. 8342–8346, 2011.